

## GRAIN ALIGNMENT BY RADIATION IN DARK CLOUDS AND CORES

JUNGYEON CHO

Department of Astronomy and Space Science, Chungnam National University, Daejeon, South Korea; jcho@cnu.ac.kr

AND

A. LAZARIAN

Department of Astronomy, University of Wisconsin, 475 North Charter Street, Madison, WI 53706; lazarian@astro.wisc.edu

Received 2005 March 1; accepted 2005 June 1

### ABSTRACT

We study alignment of grains by radiative torques. We found a steep rise in radiative torque efficiency as grain size increases. This allows the larger grains that are known to exist within molecular clouds to be aligned by the attenuated and reddened interstellar radiation field. In particular, we found that, even deep inside giant molecular clouds, e.g., at optical depths corresponding to  $A_V \lesssim 10$ , large grains can still be aligned by radiative torques. This means that, contrary to earlier claims, far-infrared/submillimeter polarimetry provides a reliable tool to study magnetic fields of prestellar cores. Our results show that the grain size distribution is important for determining the relation between the degree of polarization and intensity.

*Subject headings:* dust, extinction — ISM: clouds — polarization — radiative transfer

### 1. INTRODUCTION

It is widely believed that magnetic fields play a crucial role for the dynamics of molecular clouds and for the star formation processes (see review by Crutcher 2004 and references therein).<sup>1</sup> One of the most informative techniques of studying magnetic fields in molecular clouds is based on the use of starlight polarization and polarized emission arising from aligned dust.

Alignment of interstellar dust was not expected by theorists. Very soon after the discovery of the interstellar origin of starlight polarization by Hall (1949) and Hiltner (1949), it became clear that interstellar grains are aligned with respect to a magnetic field. It did not take a long time to realize that grains tend to be aligned with their long axes perpendicular to a magnetic field. However, progress in theoretical understanding of the alignment has been surprisingly slow, in spite of the fact that great minds such as L. Spitzer and E. Purcell worked on grain alignment (see Spitzer & Tukey 1951; Purcell 1969, 1975, 1979, hereafter P79; Purcell & Spitzer 1971; Spitzer & McGlynn 1979). The problem happened to be very tough, and a lot of relevant physics had to be uncovered. An extended discussion of different proposed mechanisms with the relevant references can be found in a recent review by Lazarian (2003).

Originally, it was widely believed that interstellar grains can be well aligned by a paramagnetic mechanism (Davis & Greenstein 1951). This mechanism, based on the direct interaction of rotating grains with the interstellar magnetic field, required magnetic fields that are substantially stronger than those uncovered by other techniques.<sup>2</sup> Later, a pioneering work by Purcell (P79)

showed a way to make grain alignment more efficient. Purcell noted that grains rotating at high rates are less susceptible to the randomization induced by gaseous collisions, while paramagnetic alignment would proceed at the same rate. He introduced several processes that are bound to make grains very fast “suprathermal” rotators. They are (1) variations of the accommodation coefficient for atoms and molecules bouncing from the grain surface, (2) variations in the coefficient of electron ejection, and (3) variations in the sites of H<sub>2</sub> formation over the grain surface. As H<sub>2</sub> formation over grain surfaces is a common interstellar process and every formation event could deposit an appreciable angular momentum with the grain, Purcell identified process 3 as the major cause of fast grain rotation. He claimed that the catalytic sites ejecting H<sub>2</sub> molecules (frequently called “Purcell’s rockets”) should spin up grains very efficiently for most of the diffuse interstellar medium (ISM). One can easily see that within the Purcell model even a small fraction of atomic hydrogen present in molecular clouds would also make them suprathermal (i.e.,  $E_{\text{kin}} \gg kT_{\text{gm}}$ ). For decades this became a standard explanation for the grain alignment puzzle, although it could not explain several observational facts, e.g., why observations indicate that small grains are less aligned than large ones.

New physics of internal grain motion uncovered fairly recently explains why small grains are poorly aligned by Purcell’s mechanism. The inefficiency stems from internal grain wobbling. Indeed, for sufficiently small grains it is impossible to assume that they rotate perfectly about their axis of maximal inertia. It is interesting to recall that the issue of grain wobbling was part of the alignment process discussed, e.g., by Spitzer (see Jones & Spitzer 1968). However, when P79 identified Barnett relaxation as a fast process of internal relaxation that aligns grain rotation with the axis of the maximal moment of inertia,<sup>3</sup> the idea that grains *always* rotate about the axis of maximal inertia became universally accepted. The flaw in this reasoning was found in Lazarian (1994), where it was shown that thermal fluctuations

<sup>1</sup> Existing claims to the contrary (see Padoan & Norlund 1999) make quantitative studies of magnetic fields more essential.

<sup>2</sup> As discussed, for instance, in Lazarian (2003), the very small grains are likely to be aligned by this mechanism, and this can explain the peculiarities of the UV part of the spectrum of the polarized radiation observed (see Kim & Martin 1995). The alignment of small grains by paramagnetic relaxation is possible because the efficiency of the Davis-Greenstein mechanism increases as the grain size decreases. The degree of alignment of small grains provides a direct constraint on the intensity of the magnetic field, which is a subject that calls for more UV polarimetry work.

<sup>3</sup> Such a rotation corresponds to the minimum of grain energy for a fixed angular momentum.

within grain material induce grain wobbling, the amplitude of which depends on the ratio of the grain rotational energy  $E_{\text{kin}}$  and  $kT_{\text{gm}}$ .<sup>4</sup> The quantitative theory of the effect presented in Lazarian & Roberge (1997) allowed revising the Spitzer & McGlynn (1979) theory of crossovers (Lazarian & Draine 1997), as well as the theory of paramagnetic alignment of thermally rotating grains (Lazarian 1997a; Roberge & Lazarian 1999).

However, a more interesting development came about later, when Lazarian & Draine (1999a, hereafter LD99a) realized that grains not only wobble but also occasionally flip. LD99a found that small grains flip more frequently than large ones. As a result, regular torques, e.g., torques due to the ejection of  $\text{H}_2$  molecules, are averaged out over flipping grains and are thermally trapped; i.e., they rotate at thermal velocities in spite of Purcell's torques. When we take into account that the paramagnetic alignment of thermally rotating grains is rather inefficient (see Roberge & Lazarian 1999), it becomes possible to explain why small grains are poorly aligned.

A new twist to the theory of grain alignment came about when Lazarian & Draine (1999b, hereafter LD99b) found that species with nuclear moments within the grain, e.g.,  $^1\text{H}$ ,  $^{13}\text{C}$ ,  $^{27}\text{Al}$ ,  $^{31}\text{P}$ ,  $^{29}\text{Si}$ ,  $^{55}\text{Mn}$ , etc., bring about a new type of internal relaxation, which was termed "nuclear relaxation." This type of relaxation for grains larger than  $10^{-5}$  cm happened to be  $\sim 10^6$  times more efficient than the Barnett relaxation introduced in P79. As the result, LD99b claimed that for diffuse interstellar gas nuclear relaxation thermally traps grains of size as small as  $10^{-5}$  cm, making the Purcell mechanism inefficient.

A group of alternative mechanisms of alignment that rely on the relative gas-grain motion have their particular niches. The first mechanical alignment mechanism was pioneered by Gold (1952). Later work included driving grains by ambipolar diffusion (Roberge & Hanany 1990; Roberge et al. 1995) and Alfvén waves (Lazarian 1994, 1997b; Lazarian & Yan 2002, 2004). Although new efficient processes of mechanical alignment have been proposed (Lazarian 1995; Lazarian & Efroimsky 1996; Lazarian et al. 1996), this did not make mechanical alignment universally applicable.

All this provided the background that made the radiative torque mechanism most promising for explaining grain alignment over vast expanses of the interstellar space. Introduced by Dolginov (1972) and Dolginov & Mytrophanov (1976), radiative torques were mostly forgotten until the pioneering work by Draine & Weingartner (1996, hereafter DW96), in which their efficiency was demonstrated using numerical simulations. The radiative torques use the interaction of radiation with a grain to spin it up. Indeed, in general, one would expect that the cross sections of the interaction of an irregular grain with left- and right-circularly polarized photons are different. As the nonpolarized light can be represented as a superposition of the equal fluxes of photons with opposite circular polarization, the interaction of such a light with the irregular grain would result in grain spin-up. Unlike Purcell's torques, which are fixed in the frame of the grain, the radiative torques are expected to be less affected by grain flipping.

The predictions of radiative torque mechanism are roughly consistent with the molecular cloud extinction and emission polarimetry (Lazarian et al. 1997) and the polarization spectrum

measured (see Hildebrand et al. 2000). They have been demonstrated to be efficient in a laboratory setup (Abbas et al. 2004). Evidence in favor of radiative torque alignment was found for the Whittet et al. (2001) data obtained at the interface of the dense and diffuse gas at the Taurus cloud (see Lazarian 2003).

In view of this success the radiative torque mechanism is the primary mechanism that we are going to study in relation to grain alignment deep inside molecular clouds. While a possible failure of radiative torques there does not exclude that grains are aligned deep within molecular clouds, their success would definitely make polarimetric studies of molecular clouds much more trustworthy and informative. To know whether grains are aligned there is necessary to know whether aligned grains trace only surface magnetic fields or magnetic fields deeply embedded in molecular clouds. The topology of the magnetic field inside molecular clouds is essential for understanding star formation.

It has been shown that optical and near-infrared polarimetry provide magnetic fields only to  $A_V$  of 2 or less (Goodman et al. 1995; Arce et al. 1998). Is it the same for far-infrared polarimetry? This is the question that we address in this paper. Earlier answers (see Lazarian et al. 1997) appeal to stars embedded in the cloud. Indeed, such stars can induce alignment through their radiation. Here we consider an extreme case, a cloud without any embedded stars. This situation is also motivated observationally, as some recent observations indicate that there are aligned grains deep in molecular clouds without high-mass stars (Ward-Thompson et al. 2000).

In what follows we discuss grain alignment by radiative torques in molecular clouds. In § 2, we calculate the efficiency of the radiative torque in a molecular cloud and the minimum aligned grain sizes as a function of the visual extinction in the cloud. In § 3, we calculate polarized far-infrared/submillimeter emission from a prestellar core and discuss the relation between the degree of polarization and the intensity. We give a discussion in § 4 and a conclusion in § 5.

## 2. RADIATIVE TORQUES

As we mentioned above, a flow of photons illuminating a grain can be represented as a superposition of left- and right-circularly polarized photons, while an irregular grain has a different cross section of interaction with photons of different handedness. As the result of differential extinction, i.e., absorption and scattering, the grain experiences a regular torque. Note that the key word here is "regular." Random torques produced by photons emitted and absorbed by a grain were discussed in terms of grain alignment by Harwit (1970). They are rather inefficient, however (Purcell & Spitzer 1971), and are more important in terms of damping the grain rotation (see Draine & Lazarian 1998).

Although the physics of grain spin-up by radiative torques was for the most part properly understood by Dolginov & Mytrophanov (1976), only calculations in DW96 provided a quantitative insight into the process. These calculations, obtained for test grains using the Discrete Dipole Approximation code (Draine & Flatau 1994), showed that both anisotropic and isotropic radiation flows can efficiently spin up grains. While Dolginov & Mytrophanov (1976) did understand that grains are not only spun up but are also aligned by anisotropic radiation, they could not correctly find what such an alignment would be. Numerical simulations in Draine & Weingartner (1997) reveal that the dynamics of grains is complex and that in most cases the grains *tend* to align with their long axes perpendicular to the magnetic field, even if paramagnetic relaxation is absent. Although the nature of this alignment in the absence of analytical calculations

<sup>4</sup> It is worth noting that the amplitude of wobbling does not decrease as the efficiency of relaxation increases. The coupling between the rotational and vibrational degrees of freedom established by the relaxation mechanism reacts to induce wobbling well in accordance with the fluctuation-dissipation theorem (see Landau & Lifshitz 1976; more discussion of this point is given in Lazarian & Yan 2004).

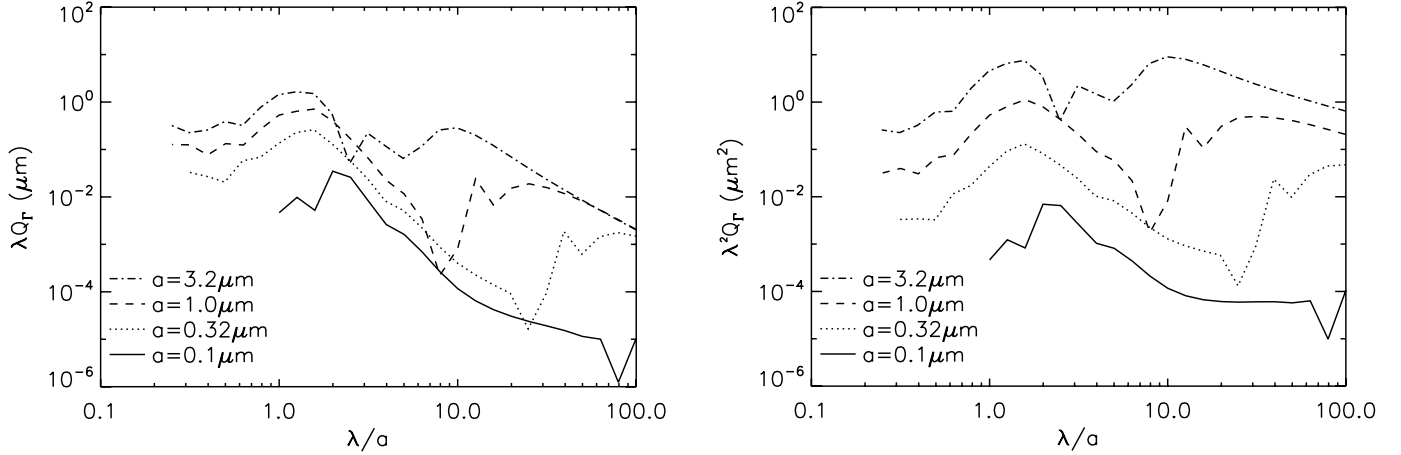


FIG. 1.—Dependence of  $\lambda|Q$  (left) and  $\lambda^2|Q$  (right) on  $\lambda/a$ , where  $\lambda$  is the wavelength and  $a$  is the grain size. These quantities are useful for estimating which part of the electromagnetic spectrum contributes most to the radiative torque.

still remains unclear and some features of grain internal dynamics (that were discovered later!) are missing in the model studied (see an attempt in this direction in Weingartner & Draine 2003), it is very plausible that radiative torques can provide the alignment that corresponds to observations. Appealing to available polarimetric data, one can claim that observations do not give us any indication that anisotropic radiation provides alignment that either has the wrong sign or depends on the angle between the magnetic field and the anisotropy direction. This would be the case, however, if the dynamics of interstellar grains was different from the assumed one. For the rest of the paper we assume that the radiative torques do align grains with their long axes perpendicular to the magnetic field, and we concentrate therefore only on the magnitude of the radiative torques.

While calculations in DW96 were limited by the relatively small grains typical to diffuse ISM, we study radiative alignment of grains of larger sizes. Such grains are known to be present in molecular clouds. In addition, unlike in DW96, here we are interested in the alignment of grains by attenuated and reddened interstellar light that enters a cloud from outside.

### 2.1. Method

We use the DDSCAT software package (Draine & Flatau 1994; DW96) to calculate the radiative torque on grain particles. We use the same grain shape as in DW96, an asymmetric assembly of 13 identical cubes. The grain is subject to a radiative torque because of its irregular shape. We use the refractive index of astronomical silicate (Draine & Lee 1984; Draine 1985; Laor & Draine 1993; see also Weingartner & Draine 2001, hereafter WD01).

In our calculations, the incoming radiation is parallel to the principal axis  $\mathbf{a}_1$  of the grain. Therefore, the target orientation angle  $\Theta$ , the angle between the incident radiation and the grains primary axis  $\hat{\mathbf{a}}_1$  (see DW96), is zero. Therefore, in our calculations the radiative torque,  $\Gamma_{\text{rad}}$ , is parallel to  $\hat{\mathbf{a}}_1$  and  $|\Gamma_{\text{rad}}| = |\Gamma_{\text{rad}} \cdot \hat{\mathbf{a}}_1|$ .

For a given wavelength and grain size, the DDSCAT package returns the torque efficiency vector  $\mathbf{Q}_\Gamma$ :

$$\mathbf{Q}_\Gamma \equiv \frac{\Gamma_{\text{rad}}}{\pi a_{\text{eff}}^2 u_{\text{rad}} \lambda / 2\pi}, \quad (1)$$

where  $\Gamma_{\text{rad}}$  is the radiative torque,  $a_{\text{eff}} \equiv (3V/4\pi)^{1/3}$  is the effective target radius (where  $V$  is the volume of the target),  $u_{\text{rad}}$  is the energy density of the incident radiation, and  $\lambda$  is the wave-

length. When we consider a radiation field with the mean intensity  $J_\lambda$ , the radiative torque becomes

$$\Gamma_{\text{rad}} = \pi a_{\text{eff}}^2 \int d\lambda (4\pi J_\lambda / c) \frac{\lambda}{2\pi} \mathbf{Q}_\Gamma, \quad (2)$$

where we used  $u_{\text{rad}} = 4\pi J_\lambda / c$ . When we perform the summation over the  $\lambda$ -axis on the natural logarithmic scale, the summation becomes

$$\Gamma_{\text{rad}} = 2.303 \Delta(\log \lambda) (a_{\text{eff}}^2 / 2c) \sum_i (4\pi J_{\lambda,i}) \lambda_i^2 \mathbf{Q}_{\Gamma,i}, \quad (3)$$

where we used  $\Delta(\log \lambda) = 2.303 d\lambda/\lambda$ . Figure 1 shows the value of  $\lambda_i |\mathbf{Q}_{\Gamma,i}|$  ( $=\lambda_i |\mathbf{Q}|$ ) and  $\lambda_i^2 |\mathbf{Q}_{\Gamma,i}|$  ( $=\lambda_i^2 |\mathbf{Q}|$ ) as a function of  $\lambda/a$  for large grains. The quantity  $\lambda_i |\mathbf{Q}_{\Gamma,i}|$  is useful for integration in equation (2), and  $\lambda_i^2 |\mathbf{Q}_{\Gamma,i}|$  is useful for integration in equation (3).

Mathis et al. (1983) showed that the average interstellar radiation field (ISRF) in the solar neighborhood consists of a small UV component plus three blackbody components with  $T = 3000$ , 4000, and 7500 K. The blackbody components are given by

$$4\pi J_\lambda \lambda = \sum_j W(T_j) 4\pi \lambda \frac{2hc^2}{\lambda^5} \frac{1}{\exp(hc/\lambda kT_j) - 1}, \quad (4)$$

where  $W(T = 3000) = 4 \times 10^{-13}$ ,  $W(T = 4000) = 1.65 \times 10^{-13}$ ,  $W(T = 7500) = 1 \times 10^{-14}$ ,  $k = 1.38 \times 10^{-16}$ , and  $h = 6.63 \times 10^{-27}$  in cgs units. See Figure 1 of Mathis et al. (1983). The radiation field inside a giant molecular cloud (GMC) located at  $r_G = 5$  kpc is also given in Figure 4 of Mathis et al. (1983). They considered a spherical GMC that has an isotropic radiation (i.e., ISRF) incident on the surface of the cloud. They produced the mean radiation intensity  $J_\lambda$  as a function of the visual extinction  $A_V$  measured from the surface of an opaque cloud. We calculate the radiative torque inside a GMC located at  $r_G = 5$  kpc using the radiation field given in Mathis et al. (1983).

Once we know  $\mathbf{Q}_{\Gamma,i}$  (from DDSCAT) and  $J_{\lambda,i}$  (from Mathis et al. 1983), we can obtain the torque from equation (3). The gas drag damps the grain angular rotation. The gas drag torque is given by

$$|\mathbf{\Gamma}_{\text{d, gas}} \cdot \hat{\mathbf{a}}_1| = (2/3) \delta n_{\text{H}} (1.2) (8\pi m_{\text{H}} kT)^{1/2} a_{\text{eff}}^4 \omega, \quad (5)$$

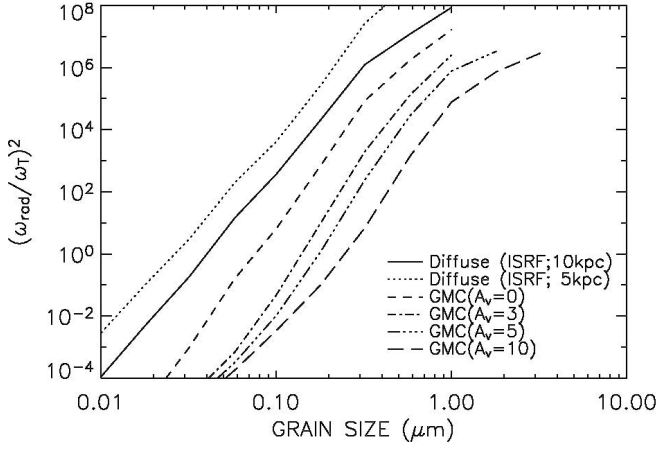


FIG. 2.—Efficiency of radiative torque. When  $\omega_{\text{rad}}/\omega_T > 1$ , radiative torque can rotate grains suprathermally, which results in grain alignment. Different curves represent radiative torque by different radiation fields. The visual extinction  $A_V$  is for a GMC located 5 kpc from the Galactic center. We assume  $n_{\text{H}} = 10^4 \text{ cm}^{-3}$  and  $T = 20 \text{ K}$  for the GMC (see Table 6 in DW96 for other parameters). For the diffuse ISM, we use  $n_{\text{H}} = 30 \text{ cm}^{-3}$  and  $T = 100 \text{ K}$  (see Table 5 in DW96).

where  $n_{\text{H}}$  is the hydrogen number density,  $m_{\text{H}}$  is the mass of a hydrogen atom,  $\delta \approx 2$ , and  $\omega$  is the angular frequency (see DW96). By equating the radiative torque  $|\Gamma_{\text{rad}}| (= |\mathbf{\Gamma}_{\text{rad}} \cdot \hat{\mathbf{a}}_1|)$  in equation (3) and the gas drag torque  $|\Gamma_{\text{d,gas}} \cdot \hat{\mathbf{a}}_1|$  above, we can obtain the angular velocity of grain rotation about  $\hat{\mathbf{a}}_1$ :

$$\omega_{\text{rad}} = \frac{|\mathbf{\Gamma}_{\text{rad}}|}{(2/3)\delta n_{\text{H}}(1.2)(8\pi m_{\text{H}}kT)^{1/2}a_{\text{eff}}^4} \left( \frac{1}{1 + \tau_{\text{d,gas}}/\tau_{\text{d,em}}} \right), \quad (6)$$

where values and definitions of the gas drag time and thermal emission drag time,  $\tau_{\text{d,gas}}$  and  $\tau_{\text{d,em}}$ , respectively, are given in DW96.<sup>5</sup>

The thermal rotation rate  $\omega_T$  is the rate at which the rotational kinetic energy of a grain is equal to  $kT/2$ :

$$\omega_T^2 = \frac{15kT}{8\pi\alpha_1\rho a_{\text{eff}}^5}. \quad (7)$$

When a grain rotates much faster than  $\omega_T$ , the randomization of a grain by gaseous collisions is reduced. Therefore, if a grain rotates suprathermally, we expect that the grain rotation axis  $\hat{\mathbf{a}}_1$  is aligned with the magnetic field. From equations (6) and (7), we have

$$\left( \frac{\omega_{\text{rad}}}{\omega_T} \right)^2 = \left[ \frac{|\mathbf{\Gamma}_{\text{rad}}|}{(2/3)\delta n_{\text{H}}(1.2)(8\pi m_{\text{H}}kT)^{1/2}a_{\text{eff}}^4} \right]^2 \times \left( \frac{8\pi\alpha_1\rho a_{\text{eff}}^5}{15kT} \right)^2 \left( \frac{1}{1 + \tau_{\text{d,gas}}/\tau_{\text{d,em}}} \right)^2, \quad (8)$$

$$= \frac{5\alpha_1}{192\delta_2} \left( \frac{1}{n_{\text{H}}kT} \right)^2 \frac{\rho a_{\text{eff}}}{m_{\text{H}}} \times \left[ \gamma \int d\lambda \mathbf{Q}_{\Gamma} \lambda (4\pi J_{\lambda}/c) \right]^2 \left( \frac{1}{1 + \tau_{\text{d,gas}}/\tau_{\text{d,em}}} \right)^2, \quad (9)$$

<sup>5</sup> Additional processes, e.g., plasma drag, were discussed in Draine & Lazarian (1998). These processes are essential for small grains but less important for the large grains that we primary deal with here.

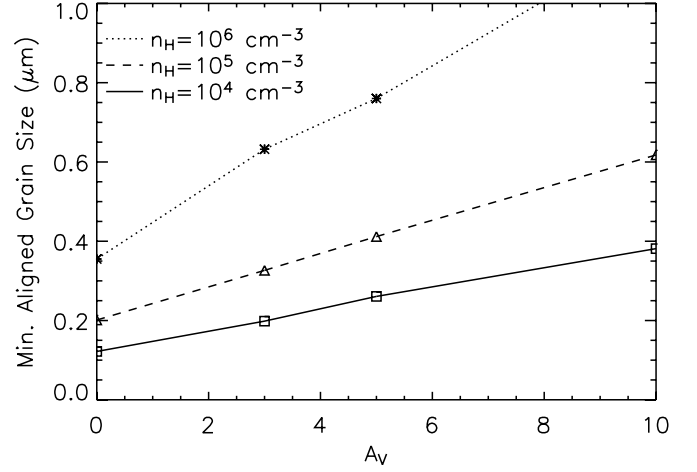


FIG. 3.—Minimum aligned grain size vs. the visual extinction  $A_V$ . We use the parameters for  $T = 20 \text{ K}$  given in DW96. However, note that we consider three different densities.

where  $\gamma$  is the anisotropy factor of the radiation field. We use  $\gamma = 0.1$  for diffuse clouds and  $\gamma = 0.7$  for the GMCs, in accordance with DW96. When the ratio is larger than 1, radiative torque is an efficient mechanism for grain alignment.

## 2.2. Results

We show the results for  $(\omega_{\text{rad}}/\omega_T)^2$  in Figure 2. The solid line is for the ISRF in the solar vicinity (see Mathis et al. [1983] for details about the radiation field). DW96 used this radiation field and obtained the  $\omega_{\text{rad}}/\omega_T$  ratio for three grain sizes ( $a_{\text{eff}} = 0.02, 0.05, \text{ and } 0.2 \mu\text{m}$ ). In their calculation, they included both isotropic and anisotropic components of the radiation field. Our calculations are slightly different. Indeed, we consider only the anisotropic radiation component, for which the effect on alignment is substantially stronger for the grain that we use than that of the isotropic component (see Table 4 in DW96).<sup>6</sup> The calculations of radiation anisotropy in a turbulent molecular cloud made for us by T. Bethel show that we do not overestimate  $\gamma$  values. On the contrary, these calculations testify that in this paper, if anything, we underestimate the actual values of radiative torques.

Another simplification is that we consider only anisotropy of radiation only along magnetic field. This is justifiable for obtaining a crude estimate, which is the actual goal of our paper. In addition, unlike DW96, we use the UV smoothed refractive index of silicon (see WD01). Nevertheless, our result (Fig. 2, *solid line*) agrees with that of DW96 within a factor of  $\sim 2$ .

In Figure 3, we show the aligned grain size as a function of the visual extinction  $A_V$ . We used Figure 2 and assumed that grains with  $\omega_{\text{rad}}/\omega_T > 5$  are aligned. For a cloud with  $n = 10^4 \text{ cm}^{-3}$ ,  $0.2 \mu\text{m}$  grains are aligned at  $A_V \sim 4$ . However, for a cloud with  $n = 10^5 \text{ cm}^{-3}$ ,  $0.2 \mu\text{m}$  grains are hardly aligned. Grains of  $\sim 1 \mu\text{m}$  are aligned even at  $A_V \sim 10$  if the density does not exceed several times  $10^5 \text{ cm}^{-3}$ .

In their classic paper, Mathis et al. (1977, hereafter MRN), constructed a model for the size distribution of dust grains in the diffuse ISM. This MRN distribution has a sharp upper cutoff at  $a_{\text{max}} = 0.25 \mu\text{m}$ . The MRN model provides a good fit to interstellar extinction and therefore is widely used for modeling the diffuse ISM. It is expected that at larger optical depths the upper cutoff occurs at larger values. For example, Kim et al. (1994) used the maximum entropy method and obtained a smooth

<sup>6</sup> We believe that this is generally true for an ensemble of grains of arbitrary shape, but more studies are necessary to prove this point.

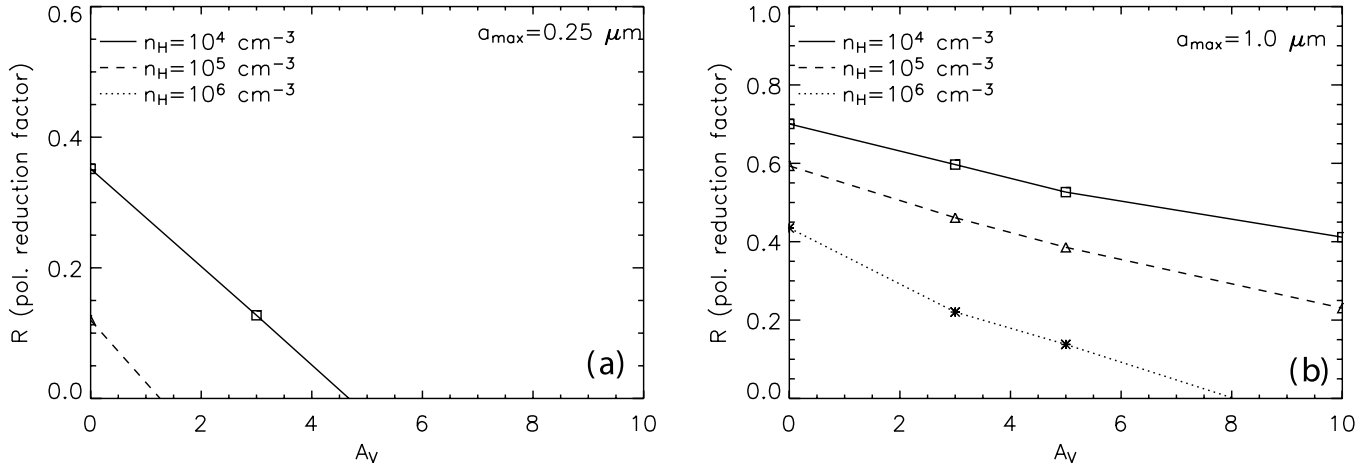


FIG. 4.—Rayleigh polarization reduction factor (see eq. [10] for the definition in our case). (a) Original MRN distribution with  $a_{\max} = 0.25 \mu\text{m}$ . (b) Extended MRN distribution with  $a_{\max} = 1.0 \mu\text{m}$ .

decrease in the size distribution starting at  $0.2 \mu\text{m}$ . WD01 also obtained an extended distribution beyond the MRN upper cutoff. Physically, coagulation of grains happens in denser parts of the interstellar gas (see discussion in Yan & Lazarian 2003; Yan et al. 2004). Therefore, it is reasonable to assume that grains larger than the usual MRN cutoff are present. Since coagulation is more frequent in dense clouds than in the diffuse ISM, we expect to see a substantial amount of grains larger than  $0.25 \mu\text{m}$  in dense clouds (see, for example, Clayton & Mathis 1988; Vrba et al. 1993). If grains of  $\sim 1 \mu\text{m}$  are abundant in dark clouds, they can emit polarized infrared radiation even deep inside the cloud.

### 2.3. Polarization: Rayleigh Reduction Factor

In Figure 4, we plot the Rayleigh polarization reduction factor  $R$  (Greenberg 1963; see also Lee & Draine 1985), which is a measure of imperfect alignment of the grain axes with respect to the magnetic field. The conventional definition of the factor is  $R = 1.5(\langle \cos^2 \beta \rangle - 1/3)$ , where  $\beta$  is the angle between the grain angular momentum vector and the magnetic field. The degree of polarization is reduced when some grains are not perfectly aligned with respect to the magnetic field. In our case this happens for an ensemble of grains, of which some, namely, the small ones, are not aligned, while others, namely, the large ones, are perfectly aligned. As the polarization for the range of far-infrared wavelengths  $\lambda$  and grain sizes  $a$  does not depend on those parameters, we can calculate the reduction factor for the entire distribution of grains as follows:

$$R = \frac{\int_{a_{\text{alg}}}^{a_{\max}} C_{\text{ran}} n(a) da}{\int_{a_{\min}}^{a_{\max}} C_{\text{ran}} n(a) da}, \quad (10)$$

where  $C_{\text{ran}}$  is the cross section,  $n(a)$  is the grain number density,  $a$  is the grain size,  $a_{\min}$  is the minimum size of the grains,  $a_{\max}$  is the maximum size, and  $a_{\text{alg}}$  is the minimum aligned size, given in Figure 3. We assume MRN-type power-law grain size distributions

$$n(a) \propto a^{-3.5} \quad (11)$$

with  $a_{\min} = 0.005 \mu\text{m}$ . We consider two values for  $a_{\max}$ , the original MRN cutoff, at  $a_{\max} = 0.25 \mu\text{m}$ , and a larger cutoff, at  $a_{\max} = 1 \mu\text{m}$ , for the calculation of  $R$ . We show the results in Figures 4a and 4b, respectively. For the original MRN distribution (Fig. 4a),  $R$  is smaller than  $\sim 0.4$  for  $n_H > 10^4 \text{ cm}^{-3}$ . How-

ever, for the larger upper cutoff (Fig. 4b),  $R$  is about  $\sim 0.2$  inside clouds at  $A_V = 10$  when  $n_H \sim 10^5 \text{ cm}^{-3}$ .

We present the results for an opaque GMC located at 5 kpc from the Galactic center. As we explained earlier, we used the radiation field given in Mathis et al. (1983). They calculated the radiation field assuming that the visual extinction  $A_V$  at the center measured from the surface is 200. However, as long as the central visual extinction is larger than  $\sim 15$ , the radiation field may not be sensitive to the choice of the central  $A_V$  (see Flannery et al. 1980). Therefore, our qualitative results obtained here are applicable to various astrophysical objects from dense prestellar cores to GMCs.

## 3. POLARIZED EMISSION FROM A DARK CORE

In § 2.3, we showed that larger grains can rotate suprathermally even at  $A_V = 10$  in GMCs. In this section, we apply this result to dense prestellar cores. As we noted at the end of § 2.3, we obtained the results in the previous section using the radiation field suitable for GMCs. Therefore, it is questionable whether or not we can directly apply the results in § 2.3 to prestellar cores. However, judging from the Flannery et al. (1980) calculation, we expect that direct application is ill-justified only near the very center of the cores.

### 3.1. Method

In this section we calculate the polarized emission from a dark prestellar core. We assume a simple spherically symmetric density distribution and a constant temperature ( $T \sim 20 \text{ K}$ ). We take the density profile of a logatropic sphere (Lizano & Shu 1989; McLaughlin & Pudritz 1996), which has a finite central density and a  $\rho \propto r^{-1}$  envelope. The logatropic sphere is supported by turbulent pressure (and isothermal gas pressure in its original form). The turbulent pressure represents nonthermal velocity dispersion observed in clouds. The density profile of a logatropic sphere is different from the critically stable isothermal Bonner-Ebert sphere (Bonner 1956; Ebert 1955), which has a  $\rho \propto r^{-2}$  envelope. Although some observations (e.g., Alves et al. 1998; Lada et al. 1999; Johnstone & Bally 1999) support the  $\rho \propto r^{-2}$  profile, other observations (e.g., van der Tak et al. 2000; Colome et al. 1996; Henning et al. 1998) support the other profile. For simplicity, we use

$$\rho(r) \propto \begin{cases} \text{const} & \text{if } r < r_0/4.7, \\ r^{-1} & \text{otherwise,} \end{cases} \quad (12)$$

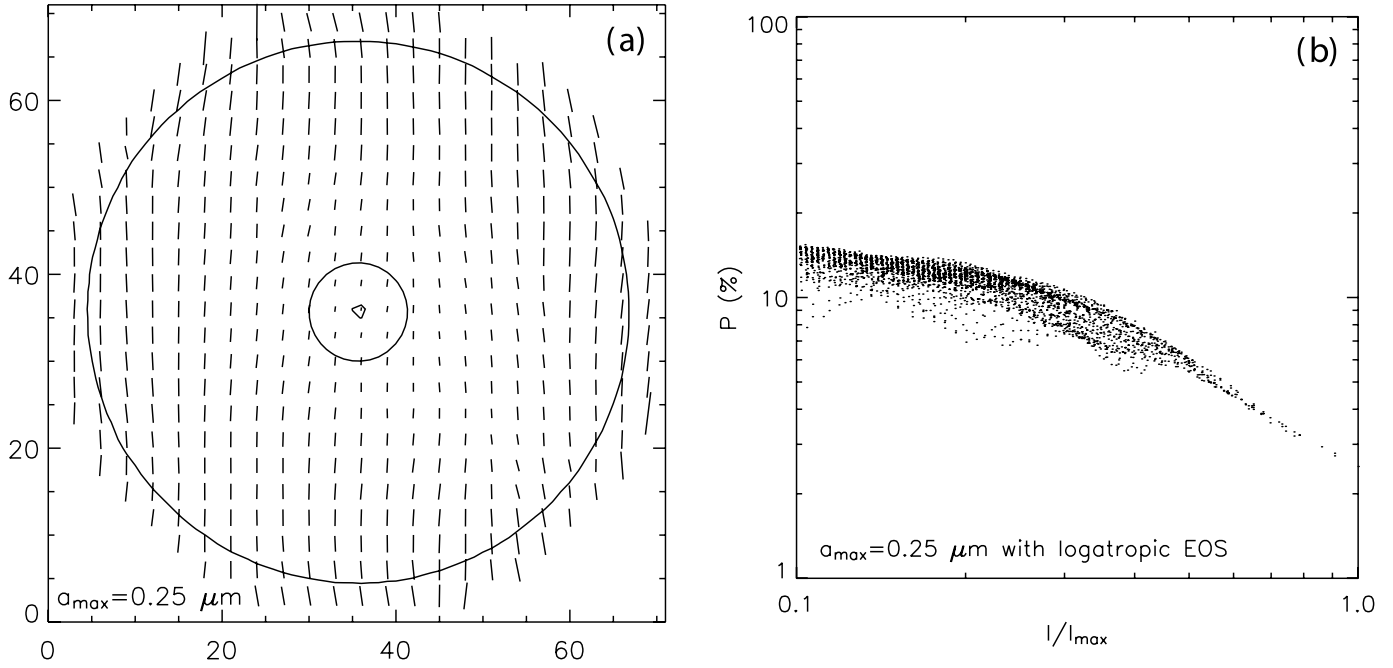


FIG. 5.—Polarization map and  $p$ - $I$  scatter diagram for the original MRN distribution (i.e.,  $a_{\max} = 0.25 \mu\text{m}$ ). We use a logotropic sphere for the density, which has a  $\rho \propto r^{-1}$  envelope. (a) From the center to the boundary, contours representing 90%, 50%, and 10% of the maximum intensity. (b) Scatter diagram following  $p \propto I^{-1}$  near the center.

where  $r_0$  is a parameter in our calculations (see McLaughlin & Pudritz [1996] for its physical meaning) and we set the central number density  $n_{\text{H},c}$  to  $3 \times 10^5 \text{ cm}^{-3}$ . This distribution truncates at  $r \sim 24r_0$ . We take the value of the magnetic field strength from our earlier direct three-dimensional numerical simulation (see Cho & Lazarian 2003). The numerical resolution is  $216^3$ , and the average Mach number is  $\sim 7$ . The magnetic field has both uniform and random components. The mean field is about 2 times stronger than the fluctuating magnetic field. We assume that the uniform field is perpendicular to the line of sight of the observer.

We assume that the visual extinction  $A_V$  at the center measured from the surface is  $\sim 10$ . This means that the total column density through the center is about  $N_{\text{H}} \sim 3.7 \times 10^{22} \text{ cm}^{-2}$ . The size of the cloud corresponds to  $\sim 0.02 \text{ pc}$ . This cloud is similar to, for example, L183 (see Crutcher et al. 2004).

We assume an MRN-type grain size distribution,  $n(a) \propto a^{-3.5}$ , from  $a = 0.005 \mu\text{m}$  to  $a = a_{\max}$ . Unlike the original MRN distribution, where  $a_{\max} = 0.25 \mu\text{m}$ , we use  $a_{\max}$  of up to  $2 \mu\text{m}$ . We assume that the grains are oblate spheroids with an axial ratio of  $\sim 1.2$ , which is smaller than the value used by Padoan et al. (2001).

We follow a method somewhat modified from the one in Fiege & Pudritz (2000) to compute the polarization maps. Here we briefly describe the procedures. It is natural to assume (see Fiege & Pudritz 2000) that one can ignore the effects of absorption and scattering when dealing with submillimeter wavelengths. Therefore, the polarization in the submillimeter range is entirely due to emission. The Stokes parameters are given by

$$Q \propto C_{\text{pol}} R q, \quad (13)$$

$$U \propto C_{\text{pol}} R u, \quad (14)$$

$$I \propto C_{\text{ran}} \left[ \int \rho ds - \frac{C_{\text{pol}} R}{C_{\text{ran}}} \int \rho \left( \frac{\cos^2 \gamma}{2} - \frac{1}{3} \right) ds \right], \quad (15)$$

where

$$C_{\text{pol}} = C_{\perp} - C_{\parallel}, \quad (16)$$

$$C_{\text{ran}} = (2C_{\perp} + C_{\parallel})/3, \quad (17)$$

$$q = \int \rho \cos^2 \psi \cos^2 \gamma ds, \quad (18)$$

$$u = \int \rho \sin^2 \psi \cos^2 \gamma ds, \quad (19)$$

$R$  is the polarization reduction factor,  $\psi$  is the angle between the projection of the local  $\mathbf{B}$  on the plane of the sky and north, and  $\gamma$  is the angle between the local  $\mathbf{B}$  and the plane of the sky. As explained earlier, the factor  $R$  is the reduction factor due to imperfect grain alignment. Note that  $a_{\text{alg}}$  is a function of both  $n_{\text{H}}$  and  $A_V$ . Figure 3 shows how  $a_{\text{alg}}$  is related to  $n_{\text{H}}$  and  $A_V$ . On the basis of the figure we assume that

$$a_{\text{alg}} = (\log n_{\text{H}})^3 (A_V + 5) / 2800 \mu\text{m}. \quad (20)$$

The error of this fitting formula is around  $\sim 10\%$ . Note that this fitting formula does not have any physical background. From  $Q$ ,  $U$ , and  $I$ , we can obtain the polarization angle  $\chi$  and the degree of polarization as follows:

$$\tan 2\chi = u/q, \quad (21)$$

$$P = \frac{\sqrt{Q^2 + U^2}}{I}. \quad (22)$$

### 3.2. Simulated Map and $p$ - $I$ Relation

In Figure 5a, we plot the polarization map for the original MRN distribution with  $a_{\max} = 0.25 \mu\text{m}$ . We clearly observe the depolarization effect; namely, the degree of polarization decreases

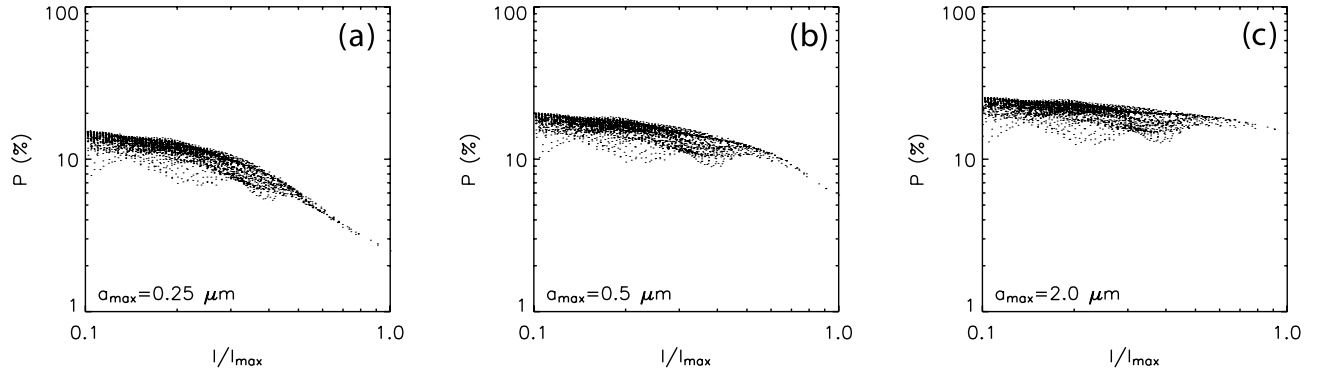


FIG. 6.—Slope becoming flatter as the upper cutoff,  $a_{\max}$ , increases. This is because a larger cutoff means that there are more aligned grains near the cloud center and therefore a higher polarization intensity. (a)  $a_{\max} = 0.25 \mu\text{m}$ , (b)  $a_{\max} = 0.5 \mu\text{m}$ , and (c)  $a_{\max} = 2.0 \mu\text{m}$ .

toward the cloud center. On the other hand, the intensity of dust IR emission is strongest at the center. Three contours represent 90%, 50%, and 10% of the maximum intensity. In Figure 5b, we plot the degree of polarization ( $p$ ) versus intensity ( $I$ ).

Many observations show that the degree of polarization ( $p$ ) decreases as the intensity ( $I$ ) increases. The relation is usually fitted by a power law. However, the exact power-law index varies. Matthews & Wilson (2000) reported  $p \propto I^{-0.7}$  for the OMC-3 region of the Orion A. On the other hand, Matthews & Wilson (2002) obtained  $p \propto I^{-0.8}$  for the dense cores in Barnard 1. For other dense cores, Henning et al. (2001) reported  $p \propto I^{-0.6}$ , Lai et al. (2003) reported  $p \propto I^{-0.8}$ , and Crutcher et al. (2004) reported  $p \propto I^{-1.2}$ . See Figure 1 of Goncalves et al. (2005) for an illustration.

We claim that the power-law index is sensitive to the value of  $a_{\max}$ . In Figure 6, we show the change of slopes as a function of the upper cutoff  $a_{\max}$ . The flattening of the slope can be understood as follows. When  $a_{\max}$  gets larger, large grains become relatively more abundant. Since larger grains are aligned even near the cloud center, we expect a higher degree of polarization

near the center. Therefore, the depolarization effect becomes less pronounced and the slope gets flatter. We leave it for further studies to establish whether or not the actual slope of the curve can be used to constrain the grain size distribution.

For the sake of completeness, we also calculate the polarization map and  $p$ - $I$  diagram for the isothermal Bonner-Ebert sphere. We take the same central density and other parameters as those in the logatropic sphere. In Figure 7a, we observe a more pronounced depolarization effect, due to a steeper density gradient. The  $p$ - $I$  scatter diagram in Figure 7b reflects this.

#### 4. DISCUSSION

Our calculations show a substantial increase of radiative torque efficiency as the grain size grows. For the power-law distribution of grain sizes we have shown that the  $p$ - $I$  relation is sensitive to  $a_{\max}$  and the density profile of clouds. The power-law distribution as an approximation of an actual grain size distribution was used only for illustrative purposes. For instance, in WD01 the grain distribution is approximated by a power law up to  $a_{\max}$  and an exponential tail of grains larger than  $a_{\max}$ . It is clear from

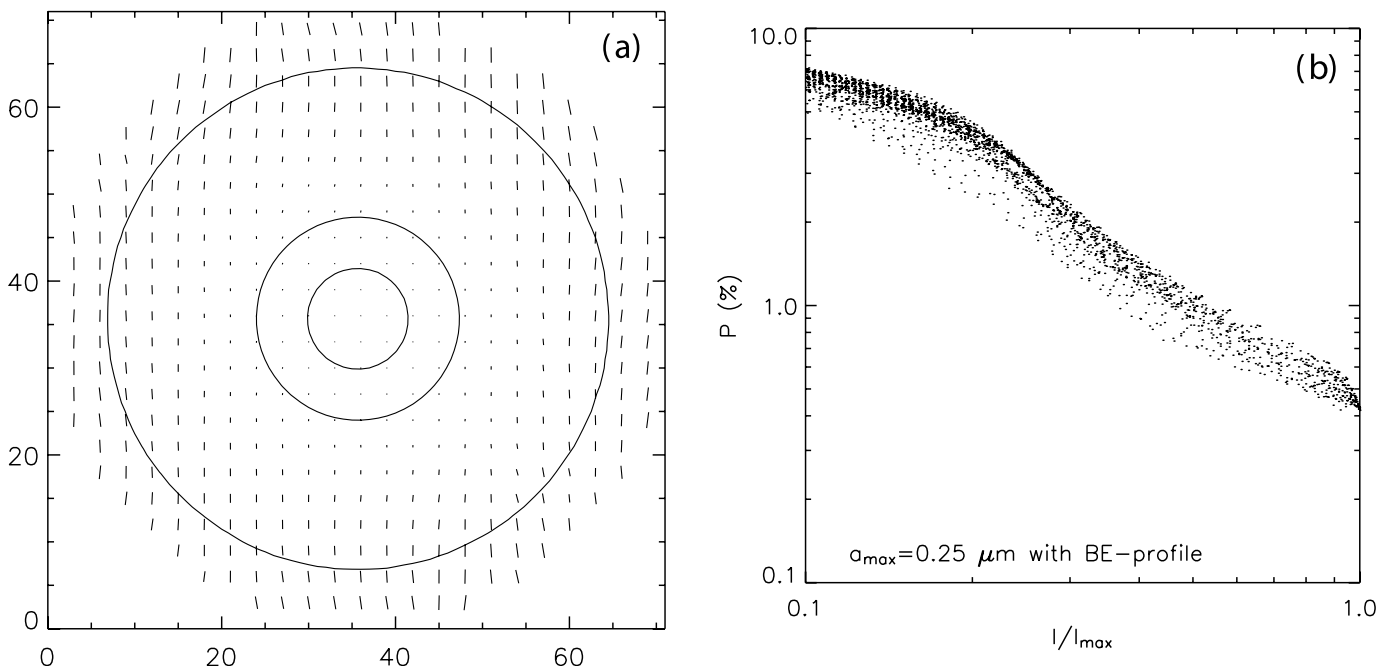


FIG. 7.—Polarization map and  $p$ - $I$  scatter diagram for the original MRN distribution (i.e.,  $a_{\max} = 0.25 \mu\text{m}$ ). We use the isothermal Bonner-Ebert sphere for the density, which has a  $\rho \propto r^{-2}$  envelope. (a) Polarization map. Contours represent 90%, 50%, and 10% of the maximum intensity. (b) Scatter diagram for the  $p$ - $I$  relation.

our calculations that if grains of size  $a_{\max}$  are aligned, the grains within the exponential tail should also be aligned. In fact, the answer to a very important question, that of whether far-infrared polarization reflects the structure of the magnetic field at high optical depths, does not depend on the details of the assumed distribution of grains. It is essential only that a substantial percentage of dust mass be in sufficiently large grains. If we want to predict a polarization spectrum (see Hildebrand et al. 2000), then the size distribution of grains does matter. For instance, grains of different sizes can have different temperatures and contribute to either the polarized or the unpolarized components of the radiation. For clouds with embedded stars, the polarization spectrum depends on the distribution of stars as well.

In practical terms, our major result is that large grains must be aligned even at high optical depths. This makes submillimeter polarimetry (see Novak et al. 2003) a useful tool for studies of magnetic fields through the entire process of star formation. An earlier understanding reflected in, for instance, Lazarian et al. (1997) was that embedded stars are essential for revealing the structure of magnetic fields at large optical depth. This meant that polarimetry might not be able to reveal the role of magnetic fields at the initial stages of star formation. It is worth mentioning that the observational evidence that grains are aligned when the radiation field is substantially reduced has recently been considered a major challenge to the grain alignment theory (see Goncalves et al. 2005).

How can we explain that the optical and near-infrared polarimetry does not detect an appreciable polarization signal originating at high optical depth? We believe that this stems from the fact that the optical and near-infrared extinction is biased toward small grains, which are not aligned. Qualitatively, the nature of the bias can be understood if one recalls that for  $\lambda < 2\pi a_c$  the efficiency of the grains in producing a polarized signal drops. At the same time, the grains with  $a > a_c$  continue to extinct light. Therefore, if a substantial number of grains are larger than  $a_c$ , the dichroic properties of the medium in terms of the transmitted light are affected only by the grains ranging in size from  $a_{\text{alg}}$ , given by equation (20), to  $\sim a_c$ . At the same time, for grain emission at  $\lambda \gg 2\pi a$  the degree of polarization is determined by the grains ranging in size from  $a_{\text{alg}}$  to  $a_{\max}$ .

To illustrate the situation in which both near-infrared and far-infrared polarimetry would show similar results, consider the grain alignment at the interface of the diffuse-dense cloud described in Whittet et al. (2001). For the range of near-infrared measurements from 0.35 to 2.2  $\mu\text{m}$  the optical cross section of grains less than 0.25  $\mu\text{m}$  is still proportional to  $a^3$ . For the Taurus Dark Clouds Whittet et al. (2001) showed that for low optical extinctions, i.e.,  $0 < A_V < 3$ , the ratio of the total to selective extinction stays similar to its value in the diffuse gas, i.e.,  $R_v \approx 3$ , while the wavelength of maximal polarization  $\lambda_{\max}$  that appears in the Serkowski law (i.e.,  $p_\lambda/p_{\max} = \exp[-K \ln^2(\lambda_{\text{exp}}/\lambda)]$ ) increases. Whittet et al. (2001) interpreted this as the result of the of size-dependent variations in grain alignment. Lazarian (2003) explained this as a consequence of radiative torques, which fail to align small grains at higher optical depths. Our results here support this conclusion. Indeed, if we adopt the grain size distribution with the original cutoff corresponding to the diffuse medium, i.e.,  $a_{\max} = 0.25 \mu\text{m}$ , using our Figure 3 and equation (10) we get a Rayleigh reduction factor (or an effective alignment) of around 10% at  $A_V = 3$ , which is a substantial reduction from the value of  $\approx 1$  for an  $A_V$  of 1.

At high optical depths the grain size distributions are rather uncertain. To illustrate the importance of the grain size growth<sup>7</sup> for alignment, let us use the distribution in WD01 corresponding to  $R_V = 5.5$  for  $A_V$  of 10 and  $n_{\text{H}} = 10^4 \text{ cm}^{-3}$ . According to Figure 3 only grains with  $a > 0.6 \mu\text{m}$  are aligned. According to WD01 the favored distribution of silicate grains is cut off at a smaller grain size. Therefore, they are not aligned. The carbonaceous grains have a distribution with a cutoff at  $\sim 1 \mu\text{m}$ . As a result, we expect  $R^{\text{carb}} \sim 0.4$ , which is larger than the value of  $A_V$  equal to 3 for effective alignment given in the previous example.<sup>8</sup> If we use another model of WD01 corresponding to  $R_V = 5.5$  that has an MRN-type distribution of carbonaceous grains up to the size  $a \sim 10 \mu\text{m}$ , then  $R^{\text{carb}}$  gets close to 0.8! With all these uncertainties we clearly see that far-infrared polarimetry can provide insight into the magnetic field topology at large optical depths. In fact, we believe that far-infrared polarimetry allows consistency checks for the models of grain size distributions.

All these results are valid for clouds without embedded massive stars. The radiation field is enhanced in the clouds, and therefore, we expect more aligned grains. If the grain size distribution stays the same as that in dark clouds, we expect to have high degrees of far-infrared polarization but still relatively little polarization in terms of optical and near-infrared polarimetry. The details of this picture can be tested using the polarization spectrum technique in Hildebrand et al. (2000).

We would claim that establishing why some grains are not aligned is as important as determining why other grains are aligned. These are two inseparable parts of the grain alignment problem that must be solved to make aligned grains a reliable technique for magnetic field study. On the basis of the present work we believe that we can account for the polarization arising from dust in dark clouds. Thermal flipping in the presence of the nuclear spin relaxation described in LD99b explains why small grains are not aligned by Purcell's torques. Therefore, we believe that we have a qualitative agreement between theory and observations (cf. Goncalves et al. 2005). We provide a qualitative comparison of the theory and observations in another paper, in which we model radiative transfer in a model of a fractal molecular cloud.

Can the alignment be higher than we predict? Yes; above we dealt only with radiative torques. In fact, calculations in LD99b show that for sufficiently large grains thermal flipping is not important. As a result, such grains are not thermally trapped and can rotate fast in accordance with Purcell's original predictions. Naturally, these grains can be aligned paramagnetically. The requirement for Purcell's torques to work in dark clouds is that a residual concentration (a fraction of 1%) of atomic hydrogen be present or that the grains have temperatures different from that of the gas. In addition, MHD turbulence can move grains mostly perpendicularly to the magnetic field lines and align them (Yan & Lazarian 2003). All these mechanisms are likely to act in unison, increasing the alignment of grains with their longer axes perpendicular to the magnetic field lines.

Our calculations are motivated by grain alignment in molecular clouds. Large grains are known to be present in accretion disks around stars, e.g., protoplanetary disks. Our work suggests that such grains should be aligned and therefore should

<sup>7</sup> It is important to realize that the increase of the upper cutoff for the grain size happens partially due to coagulation of smaller grains. Therefore, this could be achieved without mantle growth. Naturally, the models with larger grains (i.e., WD01) do not violate the dust-to-gas ratio.

<sup>8</sup> We expect to have polarization at the level of  $\approx 3\%$  for this case in emission.

reflect the structure of the magnetic field in disks. As magnetic fields are believed to play an important role in accretion, the importance of this is difficult to overestimate.

The limitation of our calculation is that we used a magnetic field from a homogeneous MHD simulation without self-gravity. In reality, the magnetic field near dense clouds can be very different from the one we used here. A recent calculation by Gonçalves et al. (2005) shows that an hourglass-type magnetic field combined with a torus-like density profile can cause depolarized emission from the cloud center. The reduction factor is around 2. Therefore, we expect further reduction of polarization when we use a more realistic magnetic field.

It is also worth mentioning that the radiation field given in Mathis et al. (1983) is based on the assumption that the cloud is spherical and uniform. Real molecular clouds are likely to be inhomogeneous and, possibly, hierarchically clumpy. As a result, the radiation has more chances to penetrate deep within molecular clouds (see Mathis et al. 2002) to allow grains to be aligned at much higher values of  $A_V$ . Elsewhere, we have obtained the radiation field inside inhomogeneous clouds using a direct numerical technique similar to the one in Bethell et al. (2004), and we intend to improve on our present work by combining our results here and a more realistic cloud model with realistic radiation field.

The ability to trace magnetic fields inside molecular clouds is difficult to overestimate. Using the Chandrasekhar & Fermi (1953) technique, one can infer the magnetic field strength in both the cloud and cloud envelope to test whether star formation takes place in subcritical or supercritical regimes (see Crutcher 2004). The magnetic connection between clouds and cloud cores is also essential for understanding the processes of star formation. Does magnetic reconnection play an important role in removing the magnetic flux from molecular clouds? This can be answered by studies of magnetic field topology. In fact, the study of magnetic topology inside molecular clouds could test different

models of magnetic reconnection, e.g., those discussed in Shay et al. (1998) and Lazarian et al. (2004). In addition, polarimetric studies of magnetic field structure can bring important insight to the structure of MHD turbulence in molecular clouds (see the review by Lazarian & Yan 2005 and references therein).

Our findings confirm that the present-day understanding of grain alignment can account for all the observational data currently available. This makes us believe that polarization arising from aligned grains has become a tool based on solid theoretical foundations. The latter is important not only for molecular cloud studies but also for many other studies, e.g., those of comets and circumstellar polarimetry (see Lazarian 2003 and references therein), as well as for predicting and interpolating to other wavelengths the polarized foreground contribution from dust (see review by Lazarian & Finkbeiner 2003 and references therein).

## 5. SUMMARY

We have studied the efficiency of grain alignment by radiative torques in optically thick clouds. We have established that the efficiency of radiative torques is a steep function of the grain size. As a result, even deep inside GMCs ( $A_V \lesssim 10$ ) large grains can be aligned by radiative torques. This means that far-infrared/submillimeter polarimetry can reliably reflect the structure of magnetic fields deep inside molecular clouds. Our results show that the grain size is important for determining the relation between the degree of polarization and the intensity from molecular cloud dust.

This work is supported by NSF grant AST 02-43156 and the NSF Center for Magnetic Self-Organization in Laboratory and Astrophysical Plasmas. This work used Canadian Institute for Theoretical Astrophysics supercomputing facilities during its early stages. We thank Bruce Draine, Dick Crutcher, Roger Hildebrand, John Mathis, and Giles Novak for useful discussions.

## REFERENCES

- Abbas, M., et al. 2004, *ApJ*, 614, 781  
 Alves, J., Lada, C., Lada, E., Kenyon, S., & Phelps, R. 1998, *ApJ*, 506, 292  
 Arce, H. G., Goodman, A. A., Bastien, P., Manset, N., & Sumner, M. 1998, *ApJ*, 499, L93  
 Bethell, T., Zweibel, E., Heitsch, F., & Mathis, J. 2004, *ApJ*, 610, 801  
 Bonner, W. 1956, *MNRAS*, 116, 351  
 Chandrasekhar, S., & Fermi, E. 1953, *ApJ*, 118, 113  
 Cho, J., & Lazarian, A. 2003, *MNRAS*, 345, 325  
 Clayton, C., & Mathis, J. 1988, *ApJ*, 327, 911  
 Colome, C., di Francesco, J., & Harvey, P. 1996, *ApJ*, 461, 909  
 Crutcher, R. 2004, in *The Magnetized Interstellar Medium*, ed. B. Uyaniker, W. Reich, & R. Wielebinski (Katlenburg-Lindau: Copernicus), 123  
 Crutcher, R., Nutter, D., Ward-Thompson, D., & Kirk, J. 2004, *ApJ*, 600, 279  
 Davis, L., & Greenstein, J. L. 1951, *ApJ*, 114, 206  
 Dolginov, A. Z. 1972, *Ap&SS*, 18, 337  
 Dolginov, A. Z., & Mytrophanov, I. G. 1976, *Ap&SS*, 43, 291  
 Draine, B. T. 1985, *ApJS*, 57, 587  
 ———. 1994, *J. Opt. Soc. Am. A.*, 11, 1491  
 Draine, B. T., & Lazarian, A. 1998, *ApJ*, 508, 157  
 Draine, B. T., & Lee, H. 1984, *ApJ*, 285, 89  
 Draine, B. T., & Weingartner, J. 1996, *ApJ*, 470, 551 (DW96)  
 ———. 1997, *ApJ*, 480, 633  
 Ebert, R. 1955, *Z. Astrophys.*, 37, 217  
 Fiege, J., & Pudritz, R. 2000, *ApJ*, 544, 830  
 Flannery, B. P., Roberge, W. G., & Rybicki, G. B. 1980, *ApJ*, 236, 598  
 Gold, T. 1952, *Nature*, 169, 322  
 Gonçalves, J., Galli, D., & Walmsley, M. 2005, *A&A*, 430, 979  
 Goodman, A., Jones, T., Lada, E., & Myers, P. 1995, *ApJ*, 448, 748  
 Greenberg, J. M. 1968, in *Nebulae and Interstellar Matter*, Vol. 7, ed. G. P. Kuiper & B. M. Middlehurst (Chicago: Univ. Chicago Press), 328  
 Hall, J. 1949, *Science*, 109, 166  
 Harwit, M. 1970, *M. Nature*, 226, 61  
 Henning, T., Burket, A., Launhardt, R., Leinert, C., & Stecklum, B. 1998, *A&A*, 336, 565  
 Henning, T., Wolf, S., Lannhardt, R., & Waters, R. 2001, *ApJ*, 561, 871  
 Hildebrand, R., Davidson, J. A., Dotson, J. L., Wovell, C. D., Novak, G., & Vaillancourt, J. E. 2000, *PASP*, 112, 1215  
 Hiltner, W. 1949, *Science*, 109, 165  
 Johnstone, D., & Bally, J. 1999, *ApJ*, 510, L49  
 Jones, R. V., & Spitzer, L., Jr. 1967, *ApJ*, 147, 943  
 Kim, S.-H., & Martin, P. 1995, *ApJ*, 444, 293  
 Kim, S.-H., Martin, P., & Hendry, P. 1994, *ApJ*, 422, 164  
 Lada, C., Alves, J., & Lada, E. 1999, *ApJ*, 512, 250  
 Lai, S.-P., Girart, J., & Crutcher, R. 2003, *ApJ*, 598, 392  
 Landau, L., & Lifshitz, E. 1976, *Statistical Physics, Part I* (2nd ed.; Moscow: Nauka)  
 Laor, A., & Draine, B. T. 1993, *ApJ*, 402, 441  
 Lazarian, A. 1994, *MNRAS*, 268, 713  
 ———. 1995, *ApJ*, 453, 229  
 ———. 1997a, *MNRAS*, 288, 609  
 ———. 1997b, *ApJ*, 483, 296  
 ———. 2003, *J. Quant. Spectrosc. Radiat. Transfer*, 79, 881  
 Lazarian, A., & Draine, B. T. 1997, *ApJ*, 487, 248  
 ———. 1999a, *ApJ*, 516, L37 (LD99a)  
 ———. 1999b, *ApJ*, 520, L67 (LD99b)  
 Lazarian, A., & Efrimsky, M. 1996, *ApJ*, 466, 274  
 Lazarian, A., Efrimsky, M., & Ozik, J. 1996, *ApJ*, 472, 240  
 Lazarian, A., & Finkbeiner, D. 2003, *NewA Rev.*, 47, 1107  
 Lazarian, A., Goodman, A. A., & Myers, P. C. 1997, *ApJ*, 490, 273  
 Lazarian, A., & Roberge, W. G. 1997, *ApJ*, 484, 230  
 Lazarian, A., Vishniac, E., & Cho, J. 2004, *ApJ*, 603, 180  
 Lazarian, A., & Yan, H. 2002, *ApJ*, 566, L105  
 ———. 2004, in *ASP Conf. Ser. 309, Astrophysics of Dust*, ed. A. N. Witt, G. C. Clayton, & B. T. Draine (San Francisco: ASP), 479  
 ———. 2005, preprint (astro-ph/0505573)

- Lee, H., & Draine, B. T. 1985, *ApJ*, 290, 211  
Lizano, S., & Shu, F. 1989, *ApJ*, 342, 834  
Mathis, J., Mezger, P., & Panagia, N. 1983, *A&A*, 128, 212  
Mathis, J., Rumpl, W., & Nordsieck, K. 1977, *ApJ*, 217, 425 (MRN)  
Mathis, J., Whitney, B., & Wood, K. 2002, *ApJ*, 574, 812  
Matthews, B., & Wilson, C. 2000, *ApJ*, 531, 868  
———. 2002, *ApJ*, 574, 822  
McLaughlin, D., & Pudritz, R. 1996, *ApJ*, 469, 194  
Novak, G., et al. 2003, *ApJ*, 583, L83  
Padoan, P., Goodman, A., Draine, B. T., Juvela, M., Nordlund, Å., & Rögnvaldsson, O. 2001, *ApJ*, 559, 1005  
Padoan, P., & Nordlund, Å. 1999, *ApJ*, 526, 279  
Purcell, E. M. 1969, *Physica*, 41, 100  
———. 1975, in *The Dusty Universe*, ed. G. B. Field & A. G. W. Cameron (New York: Watson), 155  
———. 1979, *ApJ*, 231, 404 (P79)  
Purcell, E. M., & Spitzer, L., Jr. 1971, *ApJ*, 167, 31  
Roberge, W. G., & Hanany, S. 1990, *BAAS*, 22, 862  
Roberge, W. G., Hanany, S., & Messinger, D. W. 1995, *ApJ*, 453, 238  
Roberge, W. G., & Lazarian, A. 1999, *MNRAS*, 305, 615  
Shay, M., Drake, J., Denton, R., & Biskamp, D. 1998, *J. Geophys. Res.*, 103, 9165  
Spitzer, L., Jr., & McGlynn, T. 1979, *ApJ*, 231, 417  
Spitzer, L., Jr., & Tukey, J. W. 1951, *ApJ*, 114, 187  
van der Tak, F., van Dishoeck, E., Evans, N., & Blake, G. 2000, *ApJ*, 537, 283  
Vrba, F., Coyne, G., & Tapia, S. 1993, *AJ*, 105, 1010  
Ward-Thompson, D., Kirk, J. M., Crutcher, R. M., Greaves, J. S., Holland, W. S., & Andre, P. 2000, *ApJ*, 537, L135  
Weingartner, J., & Draine, B. T. 2001, *ApJ*, 548, 296 (WD01)  
———. 2003, *ApJ*, 589, 289  
Whittet, D. C. B., Gerakines, P. A., Hough, J. H., & Shenoy, S. S. 2001, *ApJ*, 547, 872  
Yan, H., & Lazarian, A. 2003, *ApJ*, 592, L33  
Yan, H., Lazarian, A., & Draine, B. T. 2004, *ApJ*, 616, 895